SafeWind

Collaborative project funded by the European Commission under the 7th Framework Program, Theme 2007-2.3.2: Energy

"Multi-scale data assimilation, advanced wind modelling & forecasting with emphasis to extreme weather situations for a safe large-scale wind power integration"

Grant Agreement N°: 213740

Deliverable Dp-7.1

"Statistical analysis of wind power and prediction errors for selected test areas"

DOCUMENT TYPE	Deliverable
DOCUMENT NAME:	swind.deliverable_Dp-7.1_Statistical_Analysis_v1.6
VERSION:	V1.6
DATE:	2012.06.25
CLASSIFICATION:	Public
STATUS:	Final

Abstract: This document summarizes the analysis of forecasting errors in different European regions, from individual wind farms to clusters of them and to regions, i.e. control zones in the Transmission System Operator (TSO) grid. Predictability maps are introduced and evaluated based on analysis from the German Weather Service DWD. At wind farm and cluster scales, wind farms from Ireland, Northern Ireland, France and Spain are analyzed in terms of predictability versus aggregation level.

AUTHORS[1], REVIEWERS				
MAIN AUTHOR/EDITOR:	L. Frías Paredes (CENER) and N. Stoffels (ForWind)			
AFFILIATION:	CENER			
ADDRESS:	Calle Ciudad de la Innovación 7			
TEL.:	+34 948 25 28 00			
EMAIL:	lfrias@cener.com; nicole.stoffels@forwind.de			
FURTHER AUTHORS:	L. von Bremen (ForWind), J. Sanz Rodrigo (CENER)			
PEER REVIEWERS:	R. Girard (Armines)			
REVIEW APPROVAL:	Approved :		Rejected (improve as indicated below) :	
SUGGESTED IMPROVEMENTS:	*For a long list of remarks make reference to another document*			
APPROVER:				

VERSION HISTORY			
VERSION[2]:	DATE:	COMMENTS, CHANGES, STATUS:	PERSON(S):
1.2	2012-01-03	Contributions from authors submitted to Task leader	L.Frias, N. Stoffels
1.3	2012-02-06	Deliverable merged, reviewed and returned to lead authors	J. Sanz Rodrigo
1.4	2012-02-10	Deliverable sent to review	J. Sanz Rodrigo
1.5	2012-06-25	Deliverable including reviewer's comments	J. Sanz Rodrigo
1.6	2012-08-16	Header Edition	R. Girard

STATUS, CONFIDENTIALITY, ACCESSIBILITY									
STATUS:				CONFIDENTIALITY:				ACCESSIBILITY:	
S0	Approved/Released	**X**		**R0**	General public	**X**		Private web site	
S1	Reviewed			**R1**	Restricted to project members			Public web site	**X**
S2	Pending for review			**R2**	Restricted to European Commission			Paper copy	
S3	Draft for comments			**R3**	Restricted to WP members + PL				
S4	Under preparation			**R4**	Restricted to Task members +WPL+PL				

PL: *Project leader* **WPL:** *Work package leader* **TL:** *Task leader*

[1] **The authors of this document are solely responsible for its content, which does not represent the opinion of the European Community and the European Community is not responsible for any use that might be made of data appearing therein.**

[2] **VERSION NAMING : V0.x** draft before peer-review approval, **V1.0** at the approval, **V1.x** minor revisions, **V2.0** major revision

Contents

1. Introduction

Accurate forecasting of the wind resource up to two days ahead is recognised as a major contribution for reliable large-scale wind power integration. Especially, in a liberalised electricity market, prediction tools enhance the position of wind energy compared to other forms of power generation.

This document summarizes the analysis of forecasting errors in different European regions, from individual wind farms to clusters of them and to regions, i.e. control zones in the Transmission System Operator (TSO) grid. The context of this work in the Safewind project is to characterize the spatio-temporal wind power predictability in Europe and to make use of the improved predictability obtained by aggregation of wind power across Europe. The clustering or portfolio effect is a well-known technique to decrease the temporal variability of the wind fluctuations and to increase the predictability, resulting in lower imbalance costs for the TSO and higher trading benefits for the wind farm operator.

The analysis is mainly based on two forecast models: CENER's LocalPred model applied to individual wind farms and clusters of them and the German Weather Service DWD model, applied to individual wind farms, control zones in Germany and Central Europe.

From the point of view of the wind energy integration into market operation, any decrease of the prediction errors has a positive impact in the benefits because of a reduction of the deviation penalties. In this context, aggregation can help increasing the economic benefits, but only when aggregating in an optimized way. The portfolio effect is put in practice by analyzing a set of 17 wind farms situated in the Irish islands, France and Spain, i.e. covering a North-South transect where the wind climate experiences significant spatio-temporal variability. Progressive aggregation of maximally uncorrelated wind power forecasts can lead to very significant reductions in the day-ahead prediction errors.

The possibility of producing maps of wind power predictability is explored by comparing DWD forecasts with analysis data from weather service as a proxy to the observational data. This analysis-based predictability is evaluated by comparing with observations-based predictability obtained by high-resolution LocalPred predictions at two wind farms in Northern Ireland. A key aspect of predictability mapping is the use of a representative power curve and the normalization of the errors with local wind power characteristics.

The statistical analysis of wind power prediction errors presented in this report will serve as basis for the analysis of the economical value of a European-wide distributed and interconnected wind power pool, which will be the object of other tasks in WP7, summarized in [1].

2. From Individual Wind Farm to Cluster Predictability

In the electricity grid, balance must be maintained between electricity consumption and generation at any moment. Otherwise, disturbances in power quality or supply may occur. However, wind generation is a direct function of wind speed and, in contrast to conventional generation systems, it is not easily dispatchable and, therefore, fluctuations of wind generation thus receive a great deal of attention. So, managing variability of wind generation is the key aspect associated to the optimal integration of renewable energy into electricity grids.

The present study attempts to evaluate the impact of wind farm aggregations for the purpose of minimizing forecasting errors and maximizing economical benefits. Besides, it presents the first steps in the implementation of a protocol to make these aggregations in an optimal way. To this end a set of more than 100 time series of wind energy production from wind farms for the year 2008 has been used. These wind farms are sited around Ireland, France and Spain covering a North-South transect with high wind climate variability.

2.1 LocalPred wind power forecasting model

In general, a forecasting methodology like LocalPred [2][3][4][5] comprises two steps:

A. Physical modelling. Numerical weather prediction (NWP)
B. Statistical modelling. Model Output Statistics (MOS)

The Numerical Weather Prediction model predicts the real state of earth's atmosphere. The initial state of the atmosphere, so called analysis, is reproduced using a data assimilation system that integrates measurements from satellites, surface weather stations, radiosondes, etc. into a regular grid that can be used to feed a mesoscale (regional) model. By resolving the primitive equations with the input data, the NWP models can predict the weather in the future. There are different types of atmospheric models:

- Global Models: Global Forecasting System (GFS) from NCEP/NCAR and the ECMWF Global model, etc.
- Regional Models: Skiron, Eta Model, WRF, MM5, Hirlam, Aladin, etc.

LocalPred physical modeling includes SKIRON mesoscale model fed with GFS data. The NWP model SKIRON is based on the mesoscale model ETA, which has been developed at the University of Belgrade, with the main purpose of applying it to areas of irregular topography. One of its main characteristics is the use of ETA vertical coordinates instead of sigma or pressure coordinates. Its development was later continued at the National Centers for Environmental Prediction (NCEP), USA, and adapted to operational use at the Hellenic Meteorological Service (HNMS). It requires a UNIX operative system and it can use several sources of global meteorological data as boundary conditions, typically: GFS, NCEP/NCAR and ECMWF Reanalysis.

This is the basic information used by the model:

- Topographic base: 30"x30" (US Geological Survey)
- Vegetation: 10'x10' gridded data (SSiB scheme)
- Soil types: ZOBLER classification (previous conversion of UNEP/GRID Gridded FAO/UNESCO soil type units)
- SST, Snow cover and Snow depth: daily download from the NCEP analysis data.
- Input data: GFS model with 1º x 1º spatial resolution.
- Non hydrostatic configuration.

Typical datasets obtained from the SKIRON mesoscale model have the following characteristics:

- Spatial resolution 0.05º x 0.05º (approx. 4 km x 4 km depending on the latitude).
- Wind hourly simulation, including wind speed and wind direction and other meteorological parameters like air temperature and atmospheric pressure.
- Available time period: since June 2003

One of the main error sources in wind forecasts are the meteorological predictions provided by the NWP. Meteorological models solve the equations that govern the status of the atmosphere using numerical methods; therefore, initial and boundary conditions are necessary for the numerical calculations as well as digital maps of the terrain elevation and roughness. These initial conditions are defined from meteorological observations and, given the limited number of available measurement stations; they are not perfectly defined. The same holds for areas close to the boundary conditions of the mesoscale domain, where a buffer between the global and the mesoscale model creates some numerical distortion. On top of that, there is always the error due to the low resolution of the NWP which is not able to resolve some local sub-grid effects. As the complexity of the terrain increases this limitation becomes more important, and the corresponding errors larger.

In order to compensate for these errors, statistical methods have been developed to provide better forecasts. These statistical models are collectively referred to as model output statistics (MOS). MOS can correct the output for local effects that cannot be resolved by the model due to insufficient grid resolution, as well as model biases and they are based on different techniques. LocalPred contains three different MOS, two of them applied on the Skiron forecasts and the other one on the ECMWF predictions:

- MOS on Skiron forecast based on principal component analysis and multivariate regression,
- MOS on ECMWF forecast based on analogue techniques and
- MOS on SKIRON forecasts based on a set artificial intelligence techniques, so called support vector machines.

Support vector machines (SVMs) are a group of supervised learning methods that can be applied to classification or regression. They represent an extension to nonlinear models of the generalized portrait algorithm developed by Vladimir Vapnik. Support vector machines (SVMs) appeared in the early nineties as optimal margin classifiers in the context of Vapnik's statistical learning theory.

Since then SVMs have been successfully applied to real-world data analysis problems, often providing improved results compared with other techniques. The SVMs operate within the framework of regularization theory by minimizing an empirical risk in a well-posed and consistent way. A clear advantage of the support vector approach is that sparse solutions to classification and regression problems are usually obtained: only a few samples are involved in the determination of the classification or regression functions. This fact facilitates the application of SVMs to problems that involve a large amount of data. Besides, the use of kernel functions into their algorithms allows the adaptability to nonlinear problems of SVMs.

Figure 1 contains a scheme representing the total LocalPred multi-model ensemble system. We can see how it is based on two start points, GFS+Skiron and ECMWF predictions. After that, two MOS are applied to SKIRON another one is applied to ECMWF's forecasts. To finish, an ensemble module combines the three individual predictions to obtain the final one. Remark that the system is replicated in a remote site in Zamudio as a backup system.

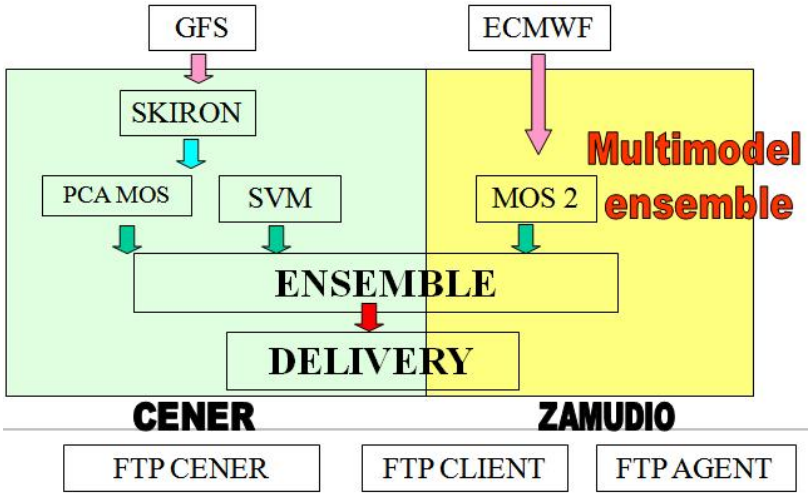

Figure 1: Description of LocalPred multi-model forecasting system

2.2 Test case description: Ireland, Northern Ireland, France and Spain

The final goal of the present study is to implement a methodology that allows us optimizing the wind farm grouping in the sense of error decreasing. To do that, power generation data from 88 wind farms are available. They are sited around Ireland, France and Spain (Figure 2). Wind power forecasts covering year 2008 have been generated by means of LocalPred system. Normalized mean absolute error (NMAE) has been used as error criteria

$$NMAE = \frac{1}{n}\sum_{i=1}^{n}\left|Pm_i - Pp_i\right| \Big/ PN$$

where *Pm* is the measured power, *Pp* the predicted power and *PN* the nominal power of the wind farm.

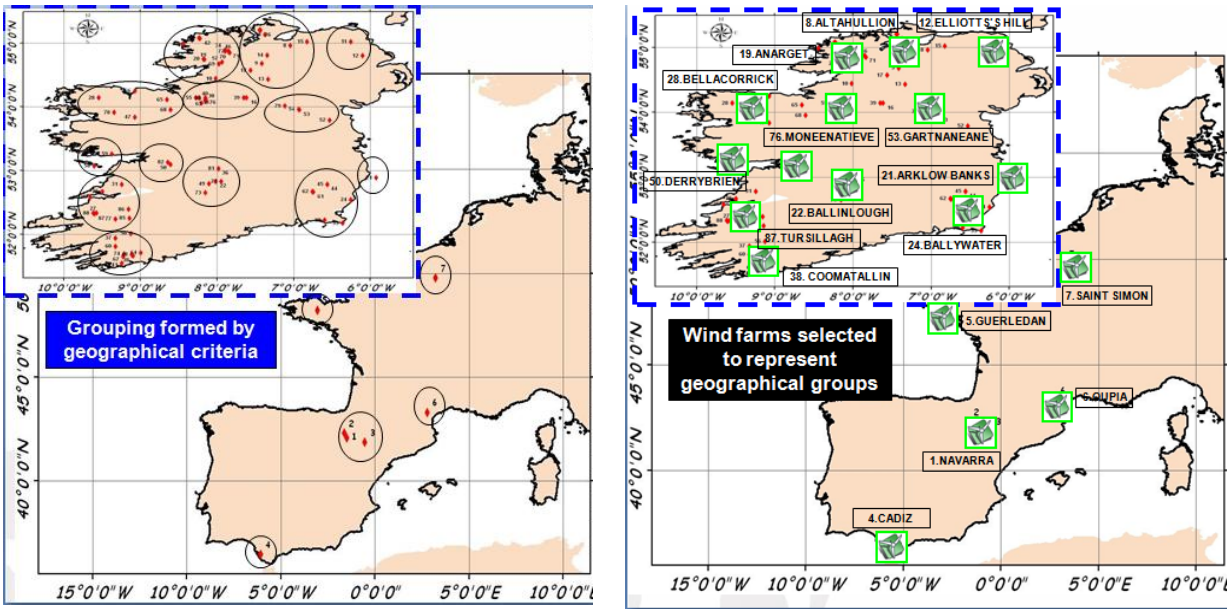

Figure 2: Available wind farms, grouping by geographical criteria and representative members

Considering the geographical distribution of all available wind farms it is supposed that the behavior of nearest emplacements have similar behavior in terms of error so, to simplify the study, we select a set of wind farms as representative of the different zones (Figure 2).

2.3 Analysis of individual forecasting errors

The forecast error of the 17 representative wind farms is presented in Figure 3. We can see how individual errors are principally sited between 10 and 16%, three of them present an error lower than 10% and two wind farms an error level greater than 16%.

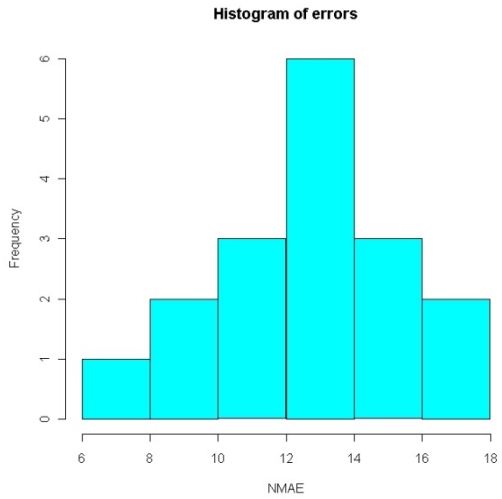

	NMAE
Altahullion	12.45
Anarget	14.28
ArklowBanks	11.4
Ballinlough	17.05
Ballywater	12.89
Navarra	13.09
Bellacorrick	10.6
Coomatallin	16.19
Cadiz	12.45
Derrybrien	10.69
Elliots Hill	13.32
Gartnaneane	13.53
Guerledan	8.25
Moneenatieve	14.83
Oupia	15.14
Saint Simon	8.89
Tursillahg	6.73

Figure 3: Forecasting NMAE errors of representative wind farms

2.4 Analysis of clustering effect across Western Europe

Individual errors of the order of 10 to 16% can be reduced by aggregation (portfolio effect). Indeed, the idea is that the more uncorrelated the wind climate between additional wind farms the lower the forecasting error after aggregation.

The analysis is first performed in Ireland, where the number of wind farms is the largest in the dataset. A first exercise is presented clustering wind farms by Irish quadrant. That is, we have divided Ireland in fourth regions (named as North East, North West, South East and South West) and we have grouped

wind farms of each region (Figure 4). The lowest error is 10.36% (SW quadrant), being similar in the rest of quadrants. However, this level of error is not significantly lower than the mean individual error observed and, therefore, it suggests that, if we want to decrease the impact of deviations, we must group Irish wind farms with other wind farms from more uncorrelated wind climates.

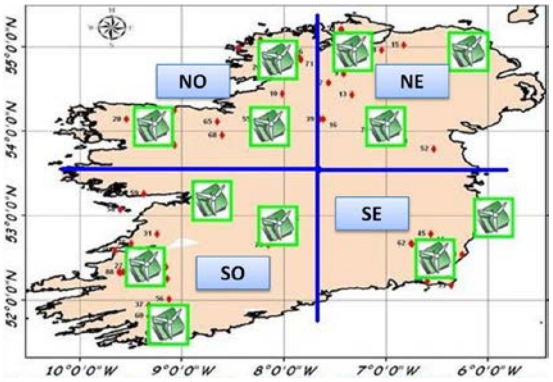

	NMAE
NE	11.97
NO	12.25
SE	11.16
SO	10.36

Figure 4: Clustering of wind farms in Irish quadrants and associated NMAE of each group

This work will analyze two key aspects of wind farm clustering. First, we will observe that a minimum error can be obtained as more wind farms are being progressively included in the cluster. Besides, an optimum clustering strategy can be defined in order to obtain an optimal error decreasing curve.

The clustering strategy is described in Figure 5. First, a representative wind farm (regarding forecasting error, nominal power and geographic situation) is chosen and its NMAE typifies the starting error level. Afterwards, we study all the possible aggregations of two wind farms with the original one, and then we consider as optimal aggregation the couple that minimizes the NMAE. This process is repeated in an iterative way: the most appropriate wind farm is included after each aggregation step.

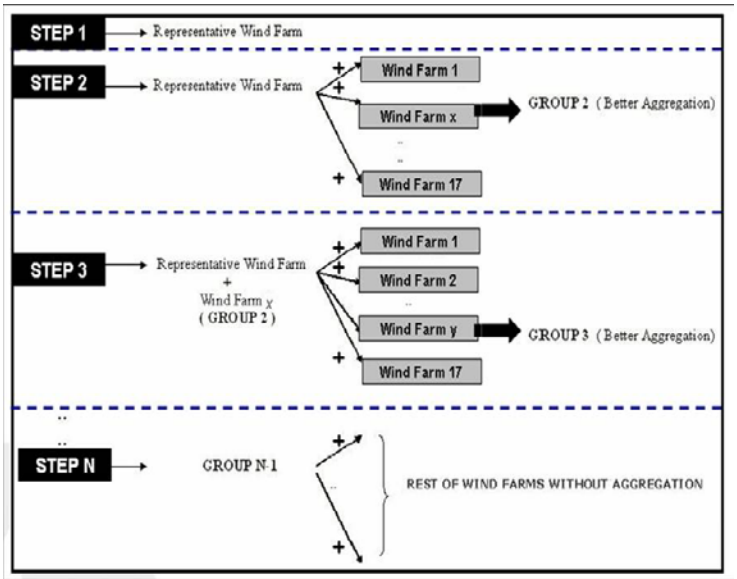

Figure 5: Diagram of clustering process

Figure 6 shows the evolution of normalized MAE in the clustering process. It can be noticed that a minimum is obtained before aggregating all the wind farms. Therefore, after a certain level, aggregation does not automatically mean error decreasing. The rate of error decreasing is very high in the first steps and levels off after the step number eleven or twelve.

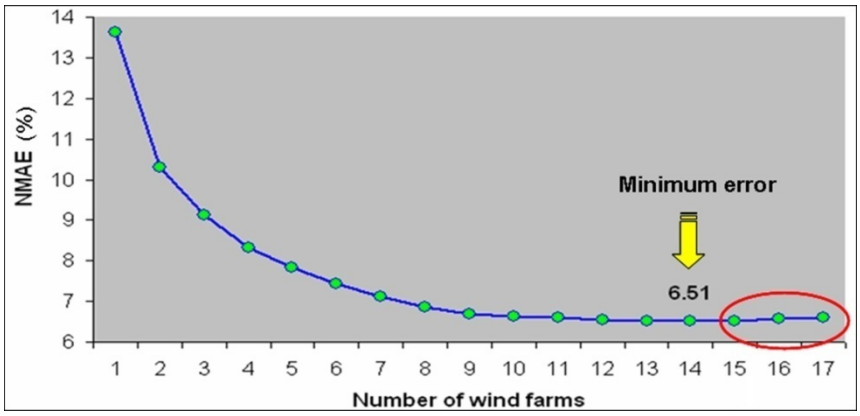

Figure 6: Evolution of normalized MAE versus the number of aggregated wind farms

To finish we show the results obtained when the procedure is only made to Irish wind farms. In these conditions the error level curve presents a similar behaviour of the whole exercise one but the potential minimal error is greater than the minimum error achieved when all wind farms are included. Both curves are plotted in Figure 7 being the red one respective to the Irish group and the blue one the whole exercise curve.

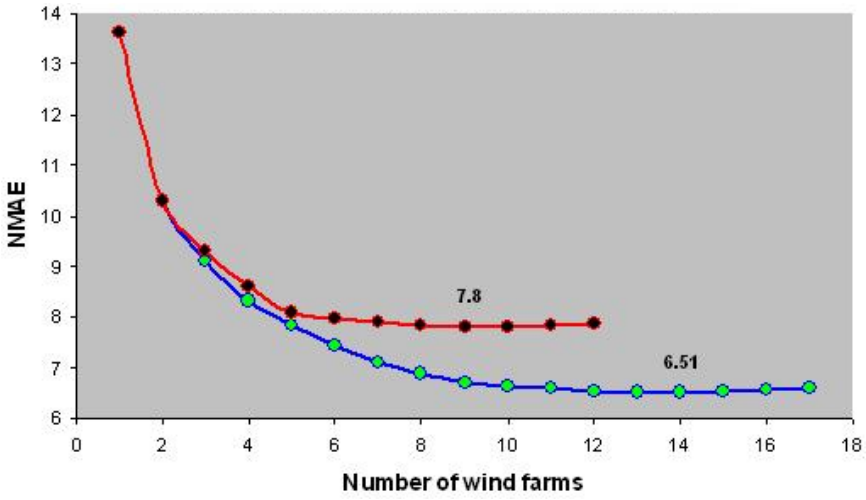

Figure 7: Evolution of NMAE considering the Irish group and the whole set of wind farms

3. From Individual Wind Farm to European-wide Predictability

For the investigation of the variability and predictability of wind power forecasts in Central Europe the COSMO-EU model from the German Weather Service DWD was utilized. The aim was to produce forecast error maps. These will serve as input in task 7.2 and 7.3 in WP7 to characterise and quantify the economic value of pool distributed wind farms. The wind energy will be sold on a common market. Due to decreased forecast errors, penalties may be avoided and the revenue increased. Predictability can then be taken as criteria for developing new wind farms.

The generation pattern and the predictability of wind power play a key role to reach the ambitious goal of a renewable energy market of 80% in 2050. While the weather cannot be influenced, the optimal spatial distribution of wind farm capacities can be estimated with historical data. The results serve as input to political frameworks in order to promote wind energy in regions with optimal spatio-temporal wind power balancing characteristics.

3.1 Test case: Central Europe

The COSMO-EU model [7] by the German Weather Service (DWD) provides forecasts and analyses on a 4.1 x 7 km grid. The domain has 490 x 297 grid points, hence 145,000 grid points in total. Forecasts are started at 00 UTC and 12 UTC; however, here only the 00 UTC forecast is considered. Forecast steps 00 – 72 are used with an hourly resolution.

The evaluation of the model was done with the DWD analysis data on the same grid. The analysis data is also available with an hourly resolution. The data covers the period 2007 and 2008. For the conversion from wind speed to wind power at 70 m height (model level 38) two different power curves were used which include losses by wake effects (Figure 8). The here used blue onshore power curve is the mean of the power curves for the Vestas V 90/2 turbine and the Enercon E 82 turbine. For comparison an offshore power curve for a small offshore wind park with 5 MW turbines is shown. The cut-off is at 25 m/s for both power curves.

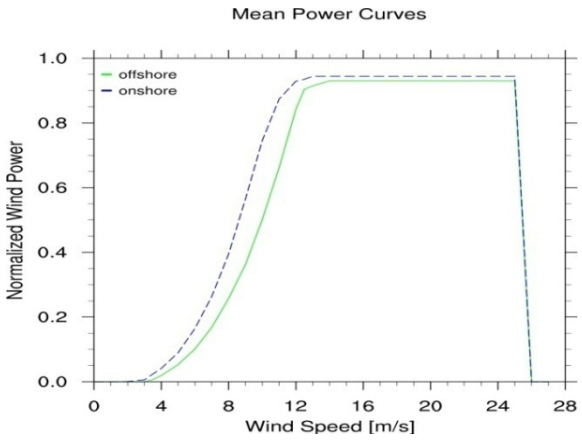

Figure 8: Wind Power Curve, the one used in the study is the blue dashed one.

The conversion from wind speed to wind power with the green offshore power curve from Figure 8 can be seen in Figure 9, with wind speed and wind power maps averaged over one year for Central Europe. N indicates the total amount of hours averaged for the plot.

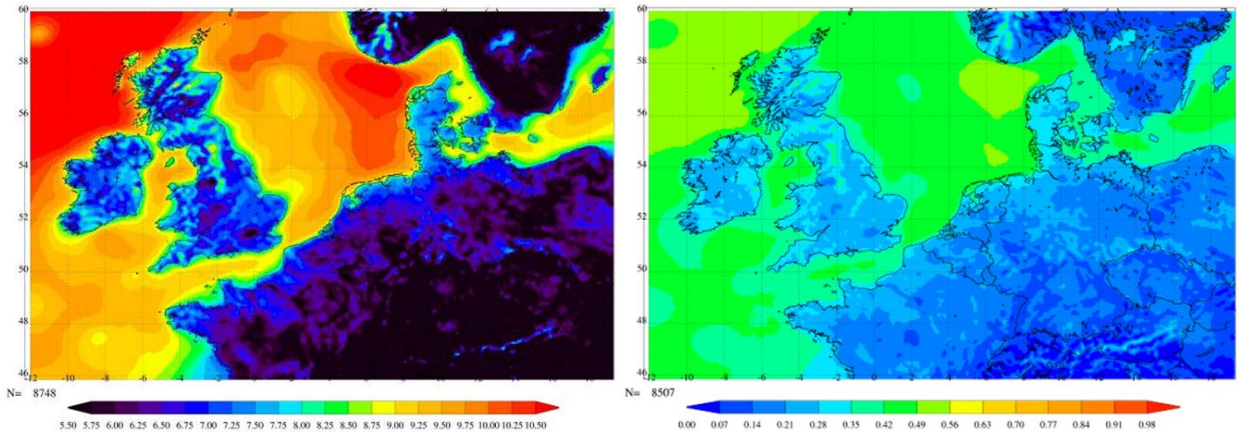

Figure 9: Mean observed wind speed in approximately 70 m in m/s (left) and resulting mean observed wind power normalised with the total installed capacity (right) for 2007.

Obviously, the high potential of offshore wind energy appears. The offshore wind power is twice the onshore wind power. Flat coastal regions are also in advance over mountain regions like the Alps.

3.2 Forecast statistics

3.2.1 Yearly statistics

The forecasts for wind power were evaluated for each of the three forecast days individually, providing statistical maps for Central Europe.

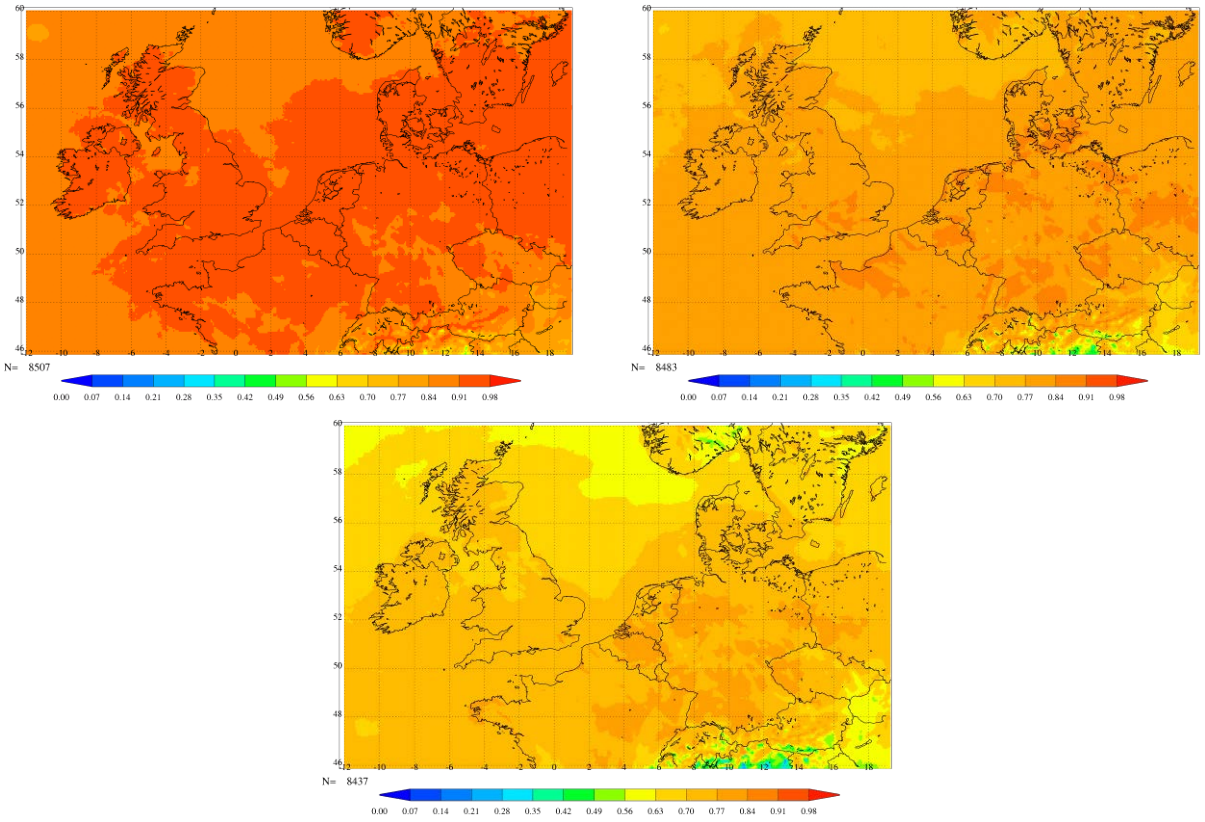

Figure 10: Correlation of forecast and analysis data for the power for forecast steps 0-24 (top left), 25-48 (top right) and 49-72 (bottom centre) for 2007.

One important question is how well the forecasts match the actual wind power analysis data. If the forecast and analysis follow the same temporal structure of high and low power values the correlation

will be high and the forecast is of good quality. For this analysis correlation maps offer a good first impression. Correlation maps for the first three forecast days are given in Figure 10.

The forecast data was correlated against the analysis data. The correlation decreases almost linearly with time in most regions. Only for the Central Europe Mountain regions and parts of Norway the decrease is faster. High correlations larger than 0.8 indicate a very good forecast quality. Offshore and Coastal regions have the best correlations over all forecast days. This was to be expected considering the higher wind speeds and the smaller roughness length over the ocean producing less turbulence and hence better forecast quality. However the single correlation is not a sufficient evidence if a model fits the analysis data or not. Hence further statistical tests have to be made.

The evolution of the $RMSE_{prod}$ (RMSE normalised with the actual produced power) over the three days is shown in Figure 11. In general the forecast error increases with forecast time. However, it becomes obvious that in some regions the error growth is faster than in other regions. For example in the mountain regions the $RMSE_{prod}$ is already large for the first forecast day and remains constant. According to the wind power production in Figure 9 these areas are not of interest anyway. Especially for the German Bight the error growth over the three days is slow compared to other offshore and onshore areas nearby. With regard to the $RMSE_{prod}$, the European coastal regions have advantages over the midland onshore regions in terms of predictability. However this is not true for Norway and Sweden where the $RMSE_{prod}$ is large for most regions, for all days.

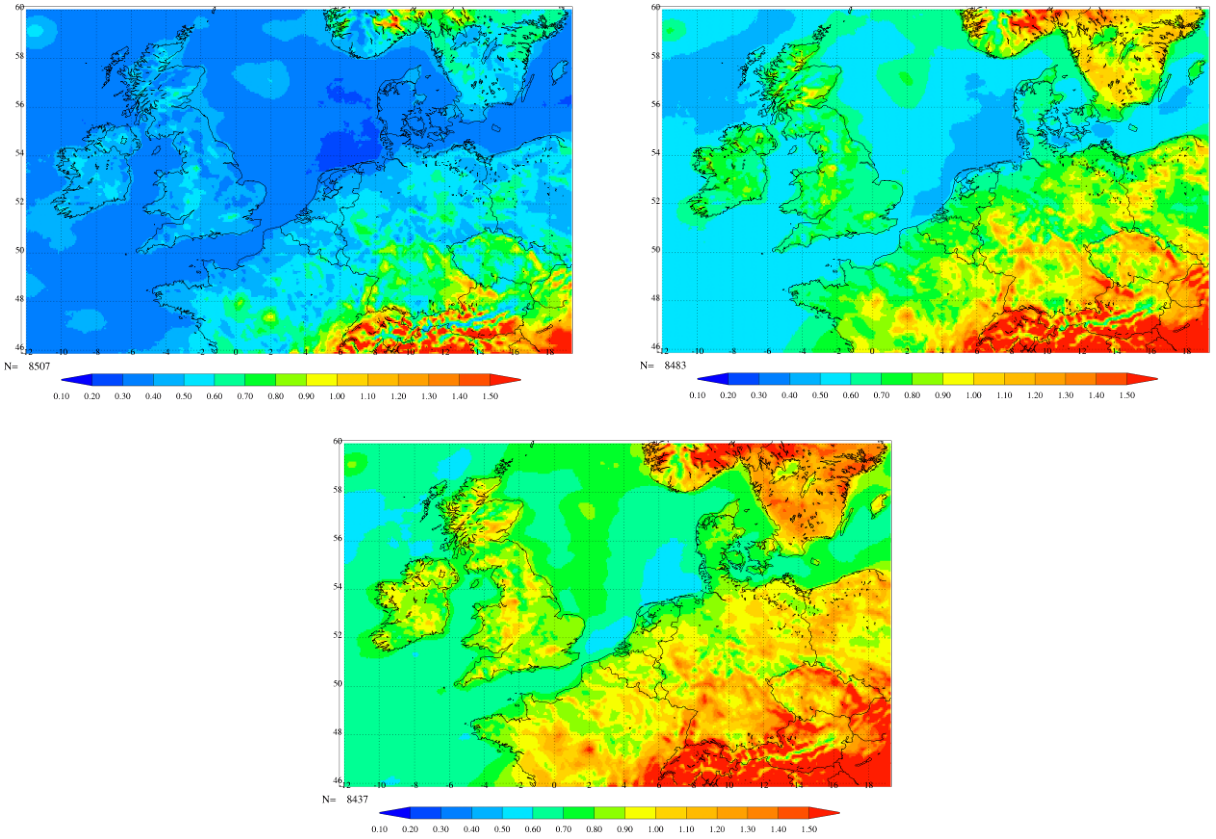

Figure 11: Mean $RMSE_{prod}$ data for the power for forecast steps 0-24 (top left), 25-48 (top right) and 49-72 (bottom centre) for 2007.

Figure 12 shows the $RMSE_{prod}$ for forecast day 3 in 2008. Basically the corresponding plot in 2007 (Figure 11) shows the same structures and only small regional differences occur. For example the $RMSE_{prod}$ in the German Bight is spatially slightly better in 2007. The same is valid for the northern part of the North Sea.

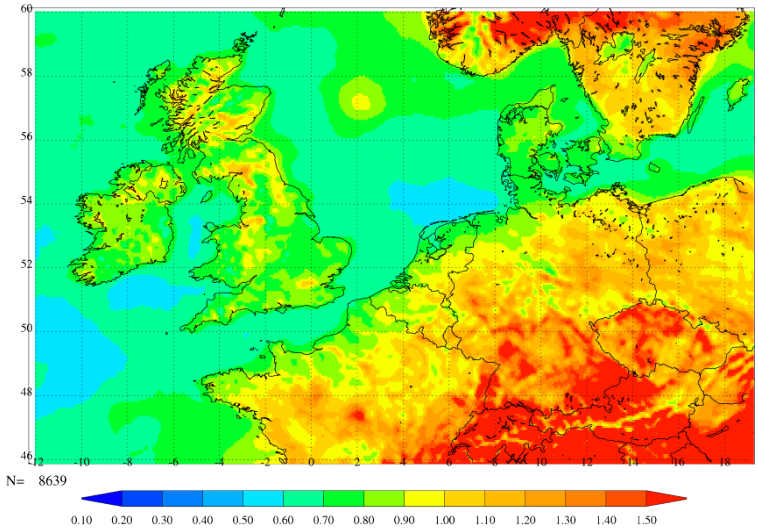

Figure 12: Mean $RMSE_{prod}$ for the power showing forecast step 49-72 in 2008.

However, as only two years were examined more years are required to conclude on interannual changes caused by e .g. climatological changes.

3.2.2 Seasonal statistics

Until now only a yearly averaged analysis was made. The question is if there are seasonal changes in the forecast statistics. Therefore the forecasts were averaged over spring (MAM), summer (JJA), autumn (SON) and winter (DJF) for the years 2007 and 2008. Especially the difference between the most contrasting season summer and winter is of interest.

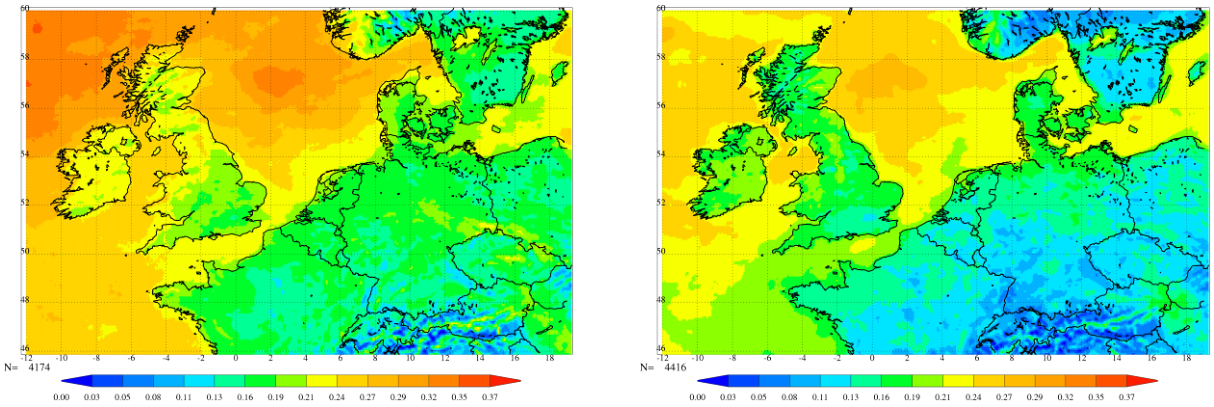

Figure 13: Mean RMSE averaged over 2007 and 2008 for winter (left) and summer (right) for the day-ahead forecast.

Figure 13 shows the RMSE of the forecast errors for the summer and winter seasons. The data was normalised with the rated capacity. The forecast error is larger offshore than onshore. Moreover the summer season shows a better RMSE than the winter season. This suggests that especially for the seasonal data a normalisation with the rated capacity is not fair since the RMSE offshore should logically be smaller than the RMSE onshore. Due to smaller turbulence and higher wind speeds over the ocean the forecasts are expected to be of a better quality.

The high seasonal differences in the energy yield cause the particular distribution of the RMSE. The DWD analysis shows that the wind power production is much higher in winter than in summer. In both seasons the offshore production is larger than the onshore production. This can be seen in Figure 14 where the load factor of the COSMO-EU analysis data is shown for both seasons.

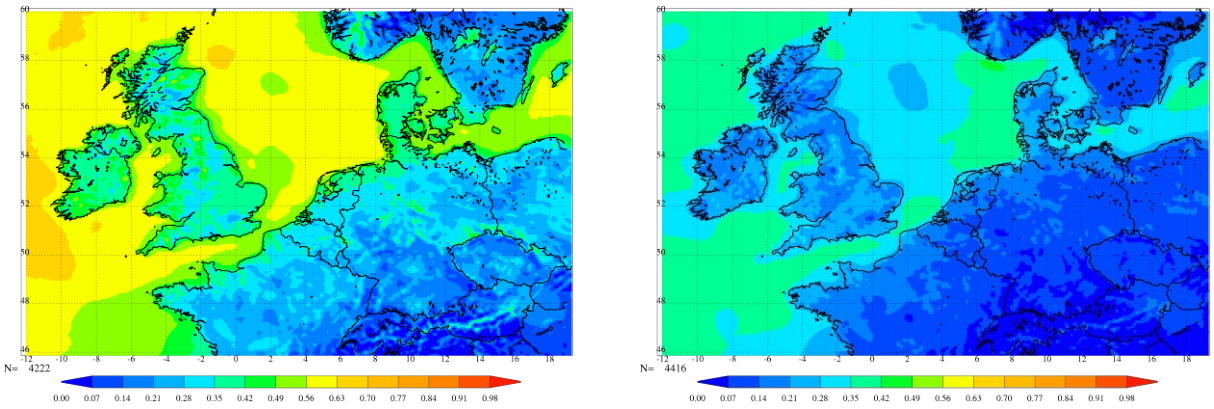

Figure 14: The mean normalised wind power production (load factor) for winter (left) and summer (right) simulated with the DWD analysis for 2007 and 2008.

A completely new method of normalisation was tried out to solve the problems with the wrong distributed RMSE. If the RMSE is divided by the actual produced wind energy instead of the installed capacity the results look completely different (Figure 15). While the yearly variation of the energy yield is rather small, the seasonal variation is extremely high. That is why this variation should be considered while analysing the seasonal data.

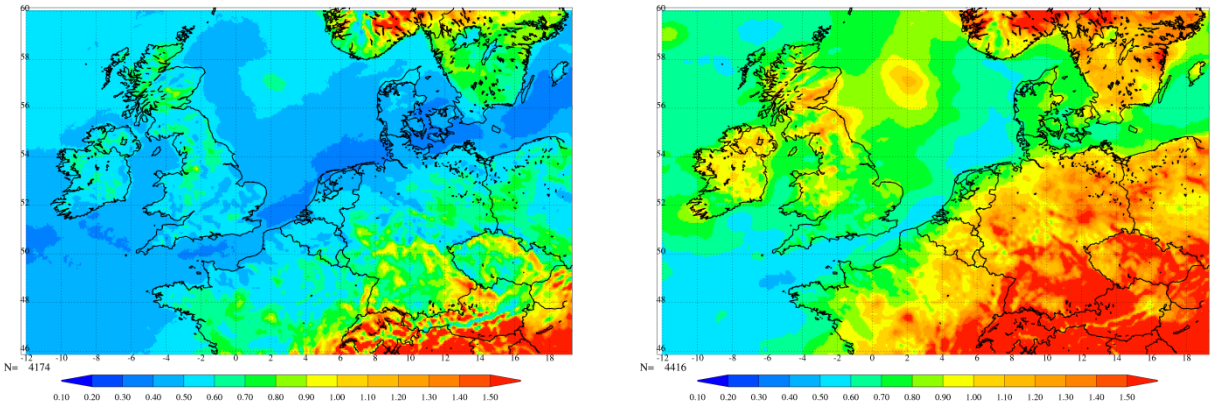

Figure 15: Mean $RMSE_{prod}$ for winter (left) and summer (right).

Normalizing against the total energy yield leads to a better RMSE in the offshore regions than the onshore regions. In summer the RMSE increases much faster inbound than in winter. In general, the forecast errors are much larger during summer than during winter. Especially in complex terrain the predictability is poorer in summer than in winter.

3.3 Evaluation of individual wind farm prediction based on COSMO-EU wind speed data

Statistical analyses are set-up to evaluate the performance of the COSMO-EU model and to compare it with existing models using a number of case studies. The synergy between statistical and physical approaches is examined to identify promising areas for further improvement of forecasting accuracy.

In order to improve the wind power prediction model from the University of Oldenburg, which is based on the Cosmo-EU model data, it was compared to the wind power prediction model developed at Cener and to the wind power prediction models used by the German Transmission System Operators (TSO). The models were evaluated against analysis data in case of the DWD data and against wind farm measurements in case of the Cener model and the TSO's commercial models. For comparison a statistical analysis was made containing correlations, standard deviations and root mean square errors as well as forecast error distributions and their statistics.

The aim is to amend the DWD model in a way that the statistical values are of the same magnitude as the statistics of the other models.

3.4 Test case: Northern Ireland

As the LocalPred model from CENER provides data from April 2008 to December 2008 the same period was used for DWD model. Only the two Northern Ireland wind farms Altahullion and Elliott's Hill were used for the analysis.

As in the previous section the DWD model data from COSMO-EU with its forecast and analysis was used. Temporal and spatial resolution are the same as in previous section. The mean wind speed was taken in 70 m for the forecast steps 00 to 48 (CENER provides a two day forecast). Once again the wind speeds were converted with the same power curve used before.

The LocalPred model is based on the Skiron NWP model, at a grid resolution of 0.1 °, and model output statistics as explained before. While the DWD model was evaluated against the DWD analysis data, LocalPred was evaluated against the SONI wind farm data for the two stations in Northern Ireland. In both cases normalised data was used for better comparison. In case of LocalPred this means that the model data was normalized with the installed capacity of the two wind farms.

As the results are quite similar for both wind farms only the results for Altahullion will be shown on the following pages.

3.5 Forecast statistics

3.5.1 Cut-Offs and Curtailment

In order to get a better impression of how far cut-offs and curtailment influence the statistical results, scatter plots of the LocalPred model data versus the wind farm data were produced. For both sites cut-offs and curtailment play a role and may influence the further statistical analysis. Hence cut-offs and curtailment are filtered out and will no longer be considered.

The cut-offs can be seen in the graphs in Figure 16. If the measured value is 0 while the forecast shows larger power values, a cut-off situation occurs. Curtailment can be seen in the SONI data as well. For 50 % of the installed power a constant measurement value can be seen while the forecast value is more than 90 %.

Figure 16 moreover shows that LocalPred forecast tends to overpredict low wind power and underpredict large wind power situations. As the scatter plot has a wide spread the forecast for a single wind farm seems to be rather vague. The COSMO-EU analysis versus the SONI measurement shows the cut-offs very clearly. But the plot is also wide spread. Even the analysis data from the DWD model differs quite a lot from the SONI measurements.

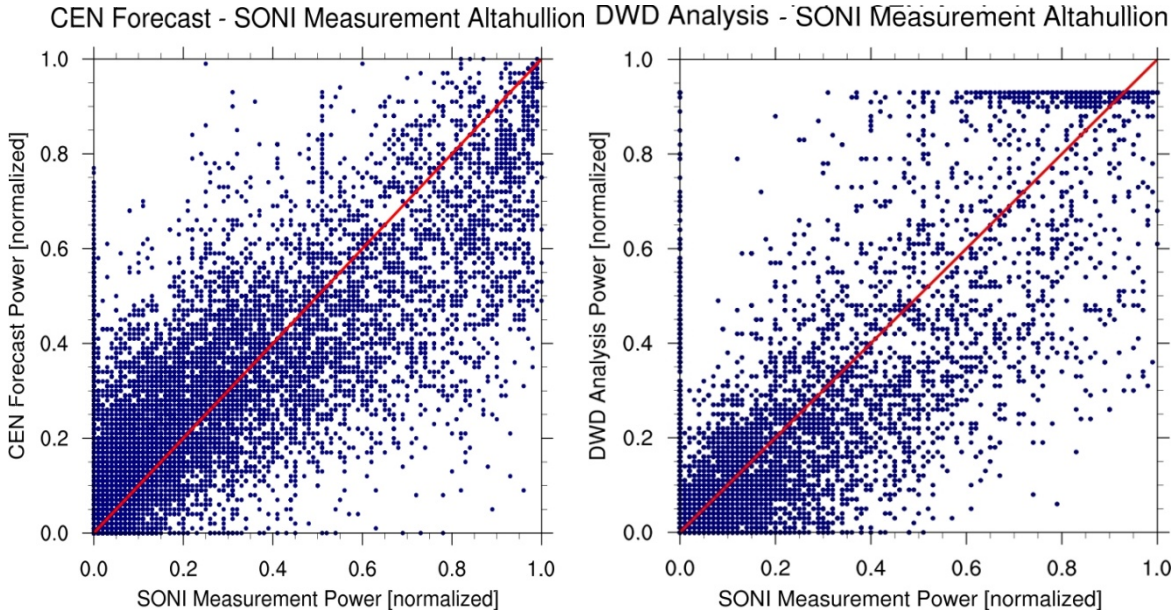

Figure 16: Scatter Plots the wind farm Altahullion for 2007 for CENER's LocalPred forecast versus the SONI measurement (left) and the COSMO-EU analysis versus the SONI measurement (right) .

3.5.2 Correlations

For statistical analysis as a first step correlations were computed. For further calculations the two forecast datasets, the measurements and the analysis datasets were merged so that forecast date, forecast hour and forecast step conform to each other. Afterwards correlations between all four datasets were produced for each month.

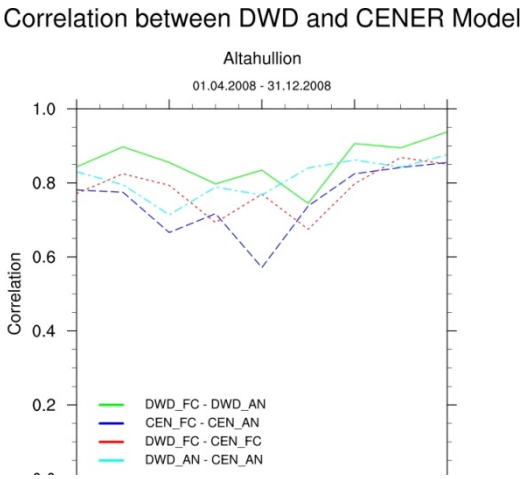

Figure 17: Monthly correlations for the wind farm Altahullion.

Large differences exist between the correlations on a seasonal basis as can be seen in Figure 17. Especially during summer LocalPred correlations have a minimum. Logically, for both sites the DWD forecast monthly correlations exceed LocalPred forecasts due to the fact that the DWD forecast was correlated with its own analysis data while the Cener forecast was correlated against independent SONI measurements. Even the correlation between the two forecasts and the two analyses are better than the correlation between the Cener model and the SONI data.

However, for further statistical analysis correlations over the whole year were produced and variances were calculated. With these two values another statistical method to find similarities between the model and the observed data can be used. The so called Taylor Plot provides information about the correlation, the ratio of the variances as well as the root mean squared error (RMSE) in one plot.

The correlation, the variances and the RMSE are related in the following way:

$$E'^2 = \sigma_f^2 + \sigma_r^2 - 2\sigma_f \sigma_r R$$

Where E'^2 is the RMSE, R is the correlation and σ_f and σ_r are the variances of the model and analysis, respectively. Based on the similarity of Law of Cosines and the above equation where the correlation is given by the cosine of the azimuthal angle a diagram can be drawn [9].

Figure 18 shows the Taylor Plot for Altahullion (red) and Elliott's Hill (blue). It differs between the DWD Forecast evaluated with the DWD Analysis (1) and the CENER's Forecast evaluated with the SONI data (2). The standard deviations on the X- and Y-axis are normalized; i. e. the ratio between the forecast standard deviation and the analysis standard deviation was calculated. A perfect ratio were analysis and forecast do not differ would be one. Hence the REF circle in the plot is the optimum value. As the correlation refers to the Pearson Correlation a value of 1 would be a perfect correlation whereas 0 means no correlation at all. The circles within the plot define the normalized RMSE in per cent, the smaller the circle the smaller the RMSE.

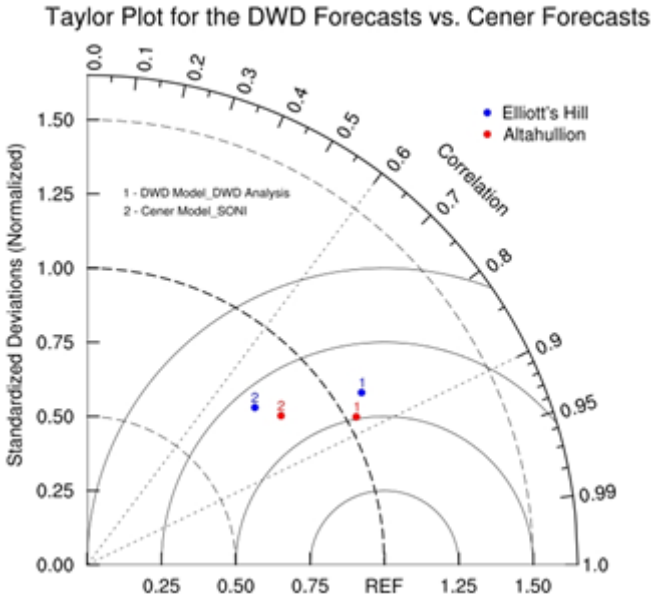

Figure 18: Taylor Plot for the two stations Altahullion and Elliott's Hill.

For both wind farms the DWD model advances CENER's model in RMSE, correlation and standard deviation. Especially Altahullion is close to the perfect standard deviation. Even more important, the statistics of the two models differ quite a lot and the standard deviation ratio is the other way around meaning that the standard deviation of the SONI data is significantly larger than the CENER model standard deviation. The differences between DWD model and DWD analysis are by far not that large. The RMSE of the DWD model is slightly better than the RMSE of the CENER model. However the differences are much smaller than for the standard deviation. The same occurs with the correlations. These results underline the tendency that could already be seen in the monthly correlations.

These differences in the performance statistics are due to the inherent differences in spatial and temporal resolution of the NWP models, the analysis data and the wind farm measurements. While the observational data include all the local effects induced by topography and wind turbine wakes, representative of scales of some meters and seconds, the analysis and NWP data can only reproduce circulation patterns down to the mesoscale level with scales of the order of kilometres and hours. Then, it is not surprising that CENER's forecasts compared with observational data results in lower performance than DWD forecasts compared with analysis data, where the resolved scales are of the same order. Besides, since DWD forecasts are forced by analysis data, the performance statistics are not based on independent data as it is the case for CENER's forecasts.

Another important quality check when evaluating the forecast quality is the RMSE. Figure 19 shows the RMSE as a function of the forecast step in per cent.

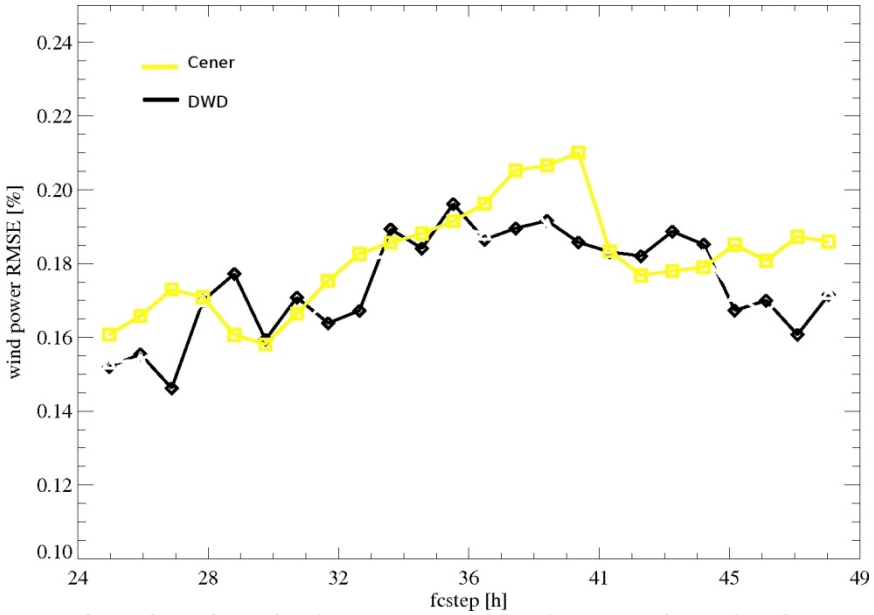

Figure 19: RMSE plotted against the forecast steps for forecast day 2 for the CENER forecast (yellow) and the DWD forecast (black).

For the DWD forecast the DWD analysis serves as reference and for the CENER forecast the SONI data. Especially the DWD RMSE is far from the expected typical linearly ascending shape typical for the COSMO model.

3.5.3 Distribution of forecast errors

Another important statistical analysis is the distribution function of the forecast errors. This includes an empirical distribution function as well as a cumulative distribution function. For the later a significance test was applied in order to find out how much the distributions of CENER and DWD differ. The Kolmogorov-Smirnov-Test provides two values, the maximum difference between the two distributions and the significance stating whether the distributions are related or not. The significance takes values between 0 and 1. For small significance values the null hypothesis has to be rejected, meaning that the similarity of the two distributions is random.

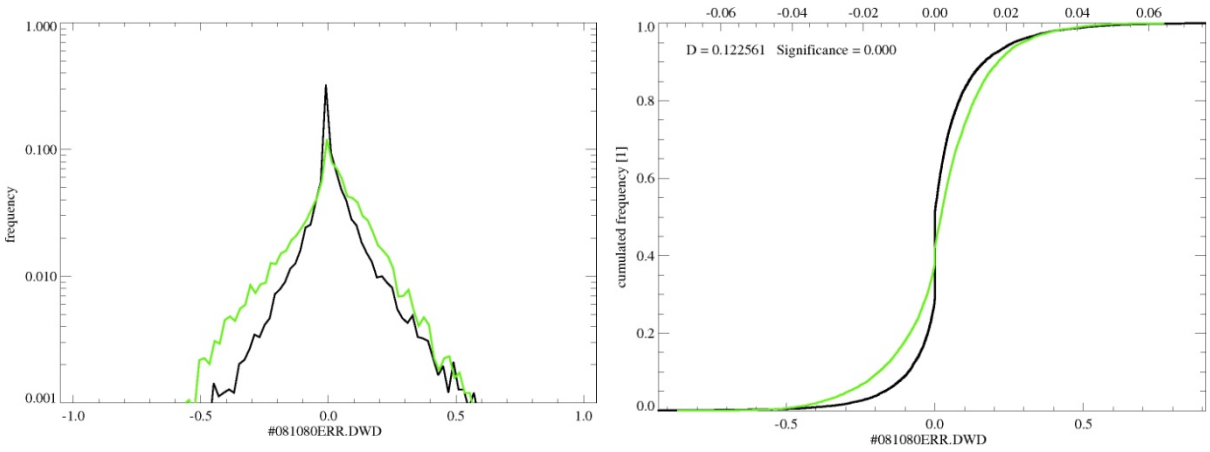

Figure 20: Empirical (left) and cumulative (right) distribution of the forecast errors for Altahullion with the DWD errors (black) and CENER errors (green).

Figure 20 shows the distributions for Altahullion. At a first glance one can see for both, the empirical and the cumulative distribution that they are not the least similar at all. This is also reflected in the significance value which is 0. Elliott's Hill shows basically the same results but Altahullion is slightly better.

The advantage of Altahullion can be explained by looking at the surrounding of the wind farm. While Elliott's Hill is based on hilly terrain, the area around Altahullion is rather flat. This leads to a roughness length of 0.01 m for Altahullion and 0.08 m for Elliott's Hill. It can be assumed that the area around Elliott's Hill is more turbulent resulting in larger forecast errors.

3.6 Evaluation of German TSO zones using linearly averaged DWD forecasts

As the forecast results for single grid points are rather poor the same analysis was done for the zones of the German Transmission System Operators (TSO): EnBW, EON (Tennet), RWE (Amprion) and Vattenfall (50 Hertz). They all provide forecast data of commercial models on their homepage.

3.6.1 Test Case: German TSO control zones

The control zones of the different TSOs can be seen in Figure 21. While the DWD data for the SONI test cases consisted only of two grid points, the closest ones to the two wind farms, the data for the German TSOs was averaged linearly over all grid points for the particular TSO area.

In total Germany has an installed capacity of approximately 27.44 GW in 2011. This leads to the following capacity shares for the single TSOs:

TSO	GW	%
EnBW	0.509	1.86
EON	10.817	39.46
RWE	4.876	17.79
VET	11.242	41.01

Table 1: Installed wind power in the German control zones (06/2011).

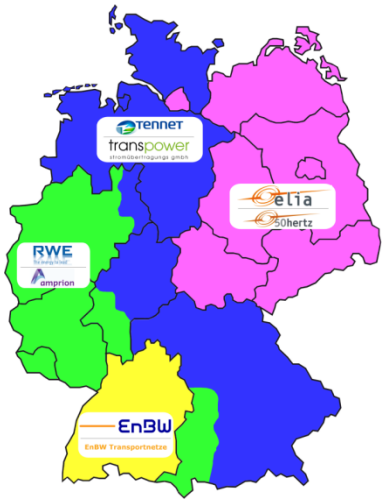

Figure 21: Control zones of the German TSOs Tennet, Amprion, 50 Hertz and EnBW (Source: http://de.wikipedia.org/wiki/Stromnetzbetreiber#Netzbetreiber)

The setup of the DWD model data is basically the same as for the DWD – CENER analysis. The data was not normalized this time due to changes in the wind power model configuration. Hence the following power values are in MW.

The data covers the period 2007 and 2008; hence it provides longer statistical analysis.

The focus of the following analysis will lie on the Tennet (EON) zone as it is Germany's largest TSO zone and the results for the other zones do not differ significantly.

3.7 Forecast statistics

3.7.1 Scatter plots

Figure 22 shows the scatter plots for the Tennet zone for the year 2007. The data was corrected with its hourly averaged bias. On the left the DWD forecast was plotted against the TSO measurements. The spreading is quite wide in contrast to the right graph were the DWD analysis was plotted against the TSO measurement. The spreading results from the higher uncertainty of the forecast. However, more important is the coving of both curves. This is due to the used power curve. The here used mean of two turbine type power curves is overestimating the wind power.

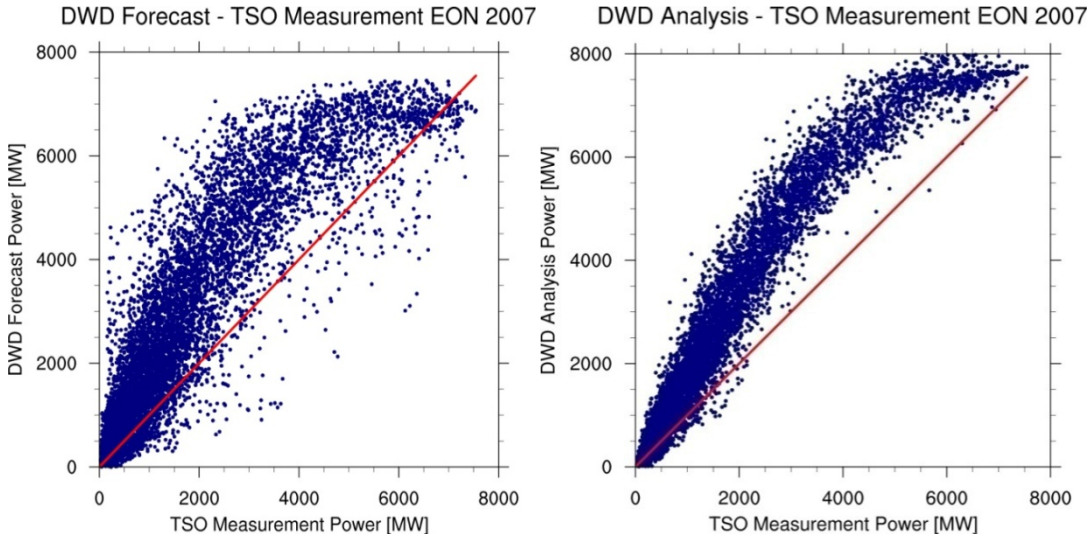

Figure 22: Scatter Plots for the DWD forecast against the TSO measurement for the day-ahead forecast (left) and the DWD analysis against the TSO measurement (right) for the Tennet zone for 2007.

3.7.2 Taylor Plot

Figure 23 shows the Taylor Plot for each TSO configuration (1-8) and for 2007 (red) and 2008 (blue). In case of the German TSO the statistics of the DWD model and the TSO models look similar except for the EnBW forecasts and the Vattenfall forecast in 2008. The later is however still adequately close to the 2nd Order statistics of the other forecast. All other forecast have the same magnitude for the statistics. Considering the scatter plot for 2008 for the EnBW forecast one can relocate the bad distribution in the Taylor Plot again. In contrast the 2007 EnBW forecast has almost the perfect forecast statistics and matches the observation very well as the ratio of the standard deviation is almost 1.

All other forecasts tend to have a larger standard deviation within the forecast than in the analysis data and measured data. But the ratios of the standard deviation are still close to 1.0 and hence satisfactory.

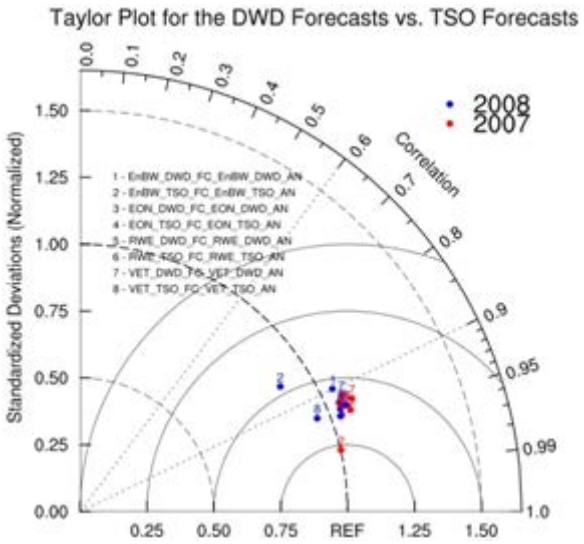

Figure 23: Taylor Plot for the German TSO models and the DWD model.

3.7.3 Forecast Errors

Figure 24 shows the cumulative forecast error distribution for the TSO Tennet for the year 2007.

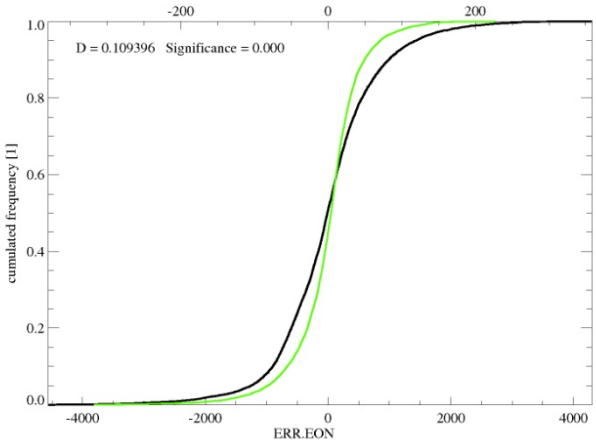

Figure 24: Cumulative distribution of the forecast errors for Tennet for 2007 (green line) and the corresponding DWD forecast (black line).

The bias corrected cumulative distribution has a different value D calculated with the Kolmogorov-Smirnov test of 0.1 which is equal to 10 % of the whole distribution. Hence the significance equals 0.0. The results for the other TSO do not differ much, except for the EnBW zone which has even larger statistical error values due to its small size and geographical position.

The RMSE is plotted against the forecast steps for the day-ahead forecast (Figure 25). The DWD forecast error is approximately 200 MW larger than the Tennet forecast. This is far too much as it is already 6 to 10 % of the installed capacity in the Tennet zone and even larger if the actually produced energy is considered.

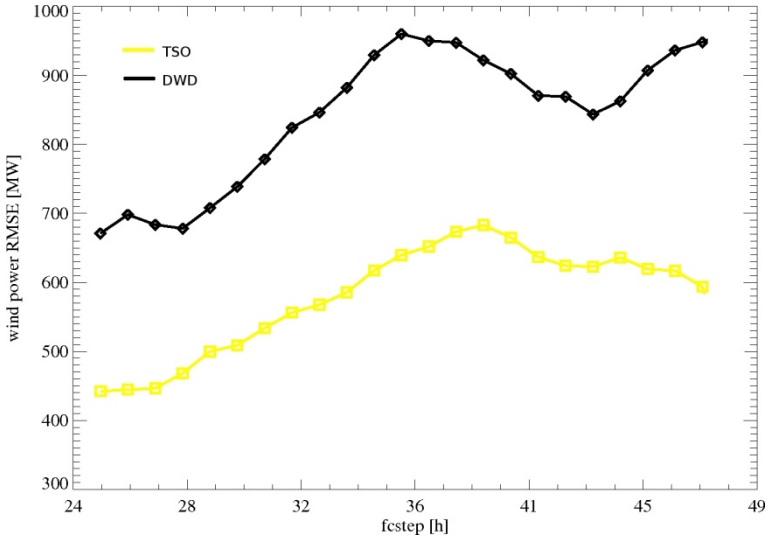

Figure 25: RMSE plotted against the forecast steps for forecast day 2 for the Tennet forecast (yellow) and the DWD forecast (black).

As none of the statistical tests brought satisfactory results which would justify using the configuration for the future analyses, other configurations of the power calculation model based on the DWD data were tested. The one with the best results is presented in the following chapter.

3.8 Evaluation of German TSO zones using weighted DWD forecasts

3.8.1 Test case: German TSO control zones

The data of the German TSO is the same as in the configuration above. The processing of the DWD data however changed significantly.

First of all the averaging over the zones changed. Now higher weights are given to grid points close to wind farms. Moreover the average hub height and the roughness length taken from the COSMO-EU model are considered while calculating the wind power.

The most important change is the power curve. In the previous chapter the scatter plots made clear that with increasing wind speed the power value grew too fast. This gave reason to try a new power curve.

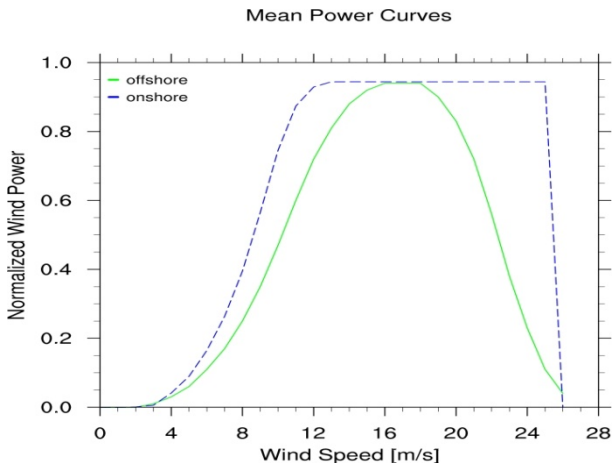

Figure 26: The power curve used in the previous chapter (blue) and the new power curve from the TradeWind project (green).

Figure 26 shows the difference between the previously used power curve and the new power curve which was developed within the framework of the TradeWind Project [8]. It does not display the power

curve for a single or as before two averaged power plants but for a region of approximately 30 km radius. The gradient of the new power curve is much smaller but closer to real measured power curves.

For easier comparison the Tennet results will be shown in the following analyses.

3.9 Forecast statistics

3.9.1 Scatter Plots

Figure 27 shows the bias corrected scatter plots for Tennet for 2007 for the new configuration. The coving of the graph is significantly smaller than with the old power curve. The DWD forecast as well as the DWD analysis is much closer to a straight line than before.

The spreading did not diminish notably. The DWD forecast is still very wide spread in comparison to the DWD analysis plotted against the SONI measurement.

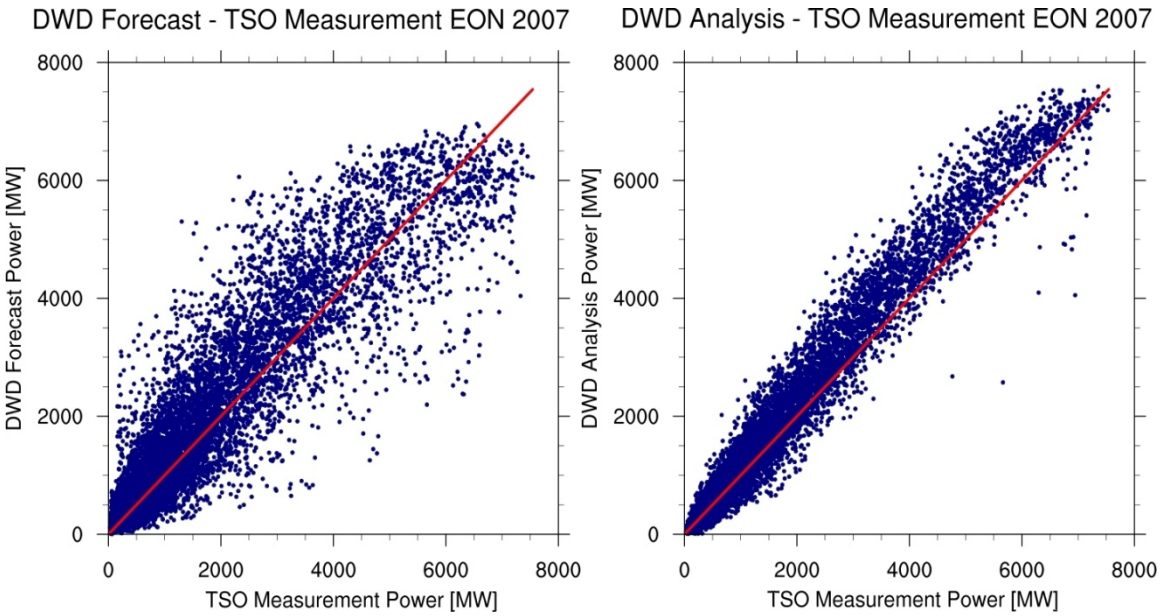

Figure 27: Scatter Plots for the DWD forecast against the TSO measurement for the day-ahead forecast (left) and the DWD analysis against the TSO measurement (right) for the Tennet zone for 2007.

3.9.2 Forecast Errors

The bias corrected data was taken to calculate the cumulative distribution. Figure 28 shows the results. The value for D could be more than bisected with the new configuration. Unfortunately the significance is still 0, so the two graphs are still far from being similar. However, the improvements of calculating the power out of the DWD wind speed are significant.

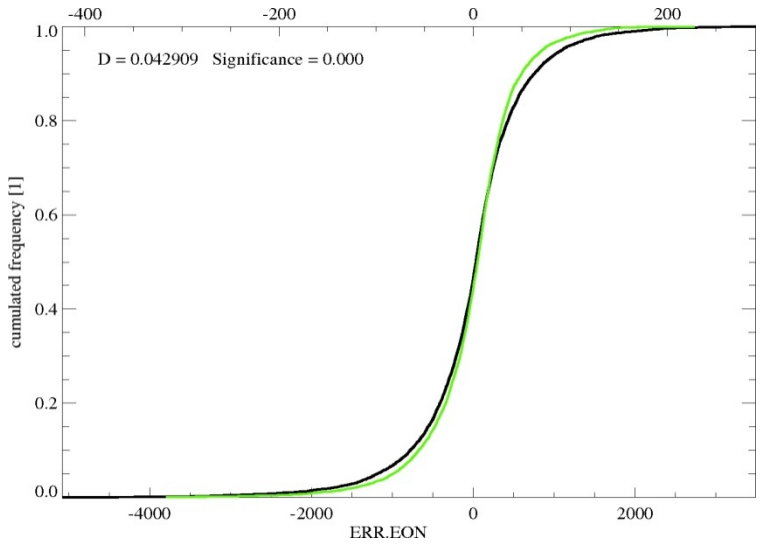

Figure 28: Cumulative distribution of the forecast errors for Tennet for 2007 (green line) and the corresponding DWD forecast (black line).

Figure 29 shows the two forecast errors plotted against each other. The plot reflects the cumulative distribution and the scatter plots. Most errors lie in the quadrant with the positive forecast errors while the quadrant with negative forecast errors contains considerably fewer points and the other two even fewer points. In the cumulative distribution a small overbalance of positive forecast errors can be seen as well.

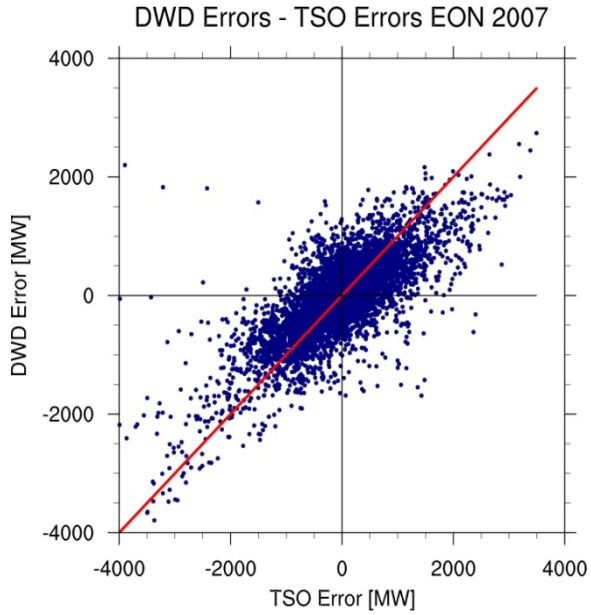

Figure 29: Scatter Plot for the forecast errors for the day-ahead forecast for Tennet in 2007.

While the RMSE depending on the forecast step was very bad for the single grid point prediction and still too large for the old configuration, a significant improvement could be made with the new configuration. Figure 30 shows the typical evolution of a RMSE with increasing ascending forecast step up to forecast step 36. The difference between the two RMSE is now half the difference of the previous configuration.

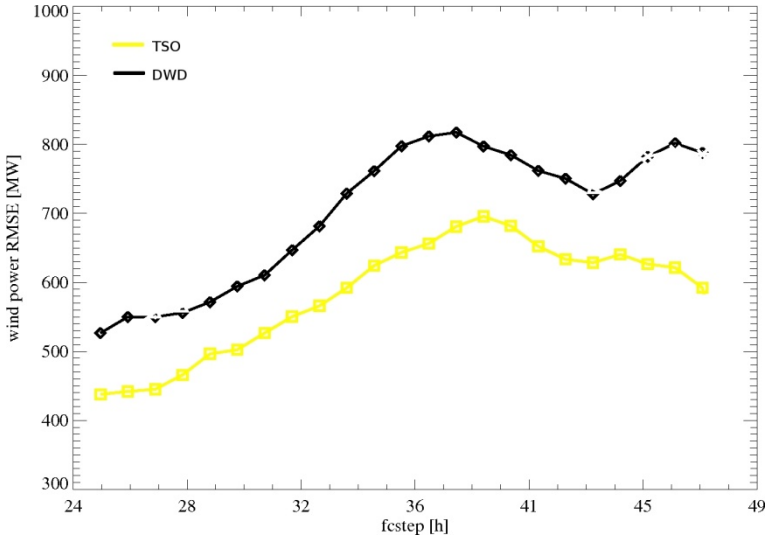

Figure 30: RMSE depending on the forecast step for forecast day 2 for the Tennet forecast (yellow) and the DWD forecast (black) for 2007.

Looking at the RMSE for the total prediction period (Figure 31) shows that the RMSE is still ascending up to forecast step 72. This does not become clear in the previous figure. Hence the saturation does not occur during the first three forecast days.

Additionally to the DWD forecast against the DWD analysis the DWD forecast against the Tennet measurement is plotted in Figure 31. As expected the RMSE is slightly larger if it is calculated with the measurement. However the gradients of both graphs are basically the same.

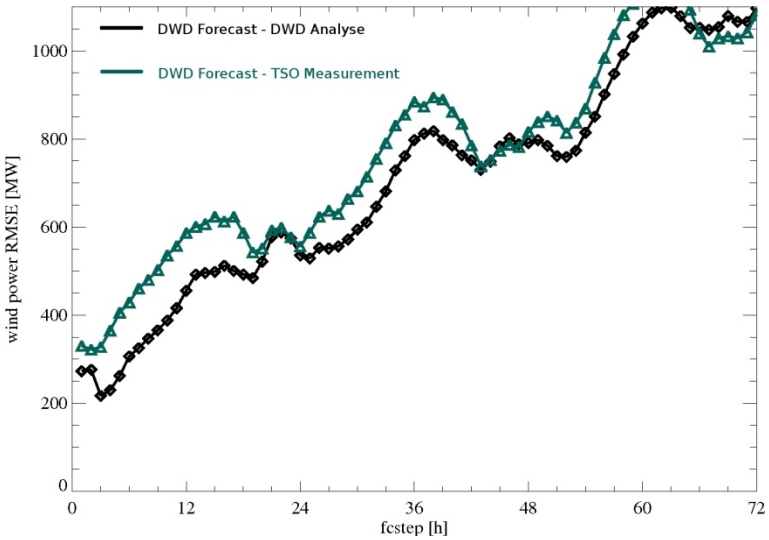

Figure 31: RMSE for forecast step 00 to 72 for the DWD forecast against the DWD analysis (black) and the DWD forecast against the Tennet measurement (green) for 2007.

4. Summary and Conclusions

This study summarizes the statistical analysis of two different approaches to wind power predictability: from individual wind farms to clusters and from individual wind farms to wide regions.

A methodology for wind farm clustering that optimized the error decreasing rate has been developed. The analysis shows that in order to achieve significant error reduction it is necessary to group wind farms from different geographical zones with highly uncorrelated wind climates. The test case analyzed shows reductions of 50% in NMAE by aggregating 10 wind farms across Western Europe.

Considering the spatial variability of wind power predictability in the EU context, offshore wind power predictability outperforms onshore predictability with respect to the same energy yield. This is the case for the yearly averaged data as well as the seasonal data. For onshore sites the predictability gets worse when the terrain is more complex. This makes especially the coastal regions favourable for wind energy development.

In terms of the seasonal model data it became clear that the normalisation of the wind power with the installed capacity is not fair, because it does not account for the seasonal changes in the load factor. Hence a normalisation of the RMSE with the mean energy yield is suggested. This is a new method of normalising wind power data and proves to create meaningful results. Regarding the seasonal dependence, wind power predictability is best in winter when normalising with the energy yield.

The comparison between the DWD model and the LocalPred showed better statistics for the DWD model. This is not surprising as the DWD analysis data was taken for validation of the DWD forecast. Only the data of two wind farms was taken for the analysis. From the DWD model the nearest grid points were taken. This causes a spatial error. Moreover the time range of only nine month does not provide reliable long term statistics for the two stations, especially if seasonal variability is considered. However, it became clear, that single grid point prediction leads to high forecast errors and bad statistics.

The situation with the German TSO zones is different from the single grid point analysis in Northern Ireland. For a first analysis two years were taken. But the TSO provides data from 2005 up to date, i.e. more years can be analysed if necessary for better long term statistics.

The data comprehends every single grid point in Germany divided into the several TSO zones. This results in a better spatial smoothing. Hence, larger zones with a homogenous distribution of wind farms have smaller forecast errors.

As the DWD model tends to overestimate the wind power production, some changes were made in the wind power model. Especially the change from the turbine specific power curve to the regional power curve helps to improve the forecast. The overestimation could be reduced significantly.

The results for this configuration still leave room for improvement as can be seen in the cumulative distribution where the significance value is still zero implying that the curves are not statistically similar. But the new configuration will serve very well for future analyses with the DWD model data such as forecast error maps or temporal gradient maps.

5. References

[1] Sanz Rodrigo, J. et al. Wind predictability as a decision factor in the resource assessment phase. Deliverable Dc7.7 of FP7-Safewind project, grant number 213740, 2012

[2] Martí, I., Nielsen, T. S., Madsen, H., et al. Prediction models in complex terrain. Proceedings of the European Wind Energy Conference. Copenhagen, July 2001.

[3] Martí, I., Usaola, J. et al. Wind power prediction in complex terrain. LocalPred and Sipreólico. Proceedings of the European Wind Energy conference, June 2003.

[4] Martí, I. et al. Wind power prediction in complex terrain: from the synoptic scale to the local scale. “The science of making torque from wind”. Delft. The Netherlands, 2004.

[5] L. Frías, M. Gastón, I. Martí .A new model for wind energy forecasting focused in the intra-daily markets. EWEC 2007.

[6] L.Frías, E.Pascal, U.Irigoyen, E.Cantero, Y.Loureiro, S.Lozano, P.M. Fernandes, I.Martí.
Support Vector Machines in the wind energy framework. A new model for wind energy forecasting. EWEC 2009.

[7] COSMO. n.d. http://www.cosmo-model.org/ (accessed 11 10, 2011).

[8] McLean, J. R. "Equivalent Wind Power Curves." TradeWind-Project, Deliverable D2.4, 2008.

[9] Taylor, K. E. "Summarizing multiple aspects of model performance in a single diagram." J. Geophys. Res. , 2001: 7183-7192.